

Optically Controlled Metamorphic Antenna

B J Hughes, I C Sage, G J Ball
QinetiQ Ltd, St Andrews Rd, Malvern, Worcestershire WR14 3PS, UK

Abstract

The suitability of photoconducting semiconductors for switches in metamorphic (reconfigurable) segmented antennas was investigated. Optically activated switches offer the benefit that metallic bias lines, which could affect antenna performance if included on the antenna plane, are not required. Bowtie antennas were designed and modelled; results indicating a broad frequency coverage, formed from switching between narrower contiguous bands, were obtained. First simple evaluation structures incorporating photoconducting semiconductors were designed and fabricated. Optically activated changes in microwave properties (S_{11} and S_{12}) were measured.

Introduction

This paper summarises work from the second year of an EMRS DTC project on metamorphic antennas. Work in the first year was based on an antenna concept comprising a photoconducting layer behind which is a pixellated light source. The pixellated light source is addressable and reconfigurable, creating different patterns of high conductivity on the photoconductor. These define different antenna shapes, to give changeable antenna properties [1].

Work focussed on establishing the attainable performance of photoconducting layers and comparing it against the needs of optically addressed metamorphic antennas. This was undertaken by: (a) fabricating and assessing photoconducting CdS/CdSe layers; (b) defining the performance needed from the photoconductor through electromagnetic modelling.

It was concluded that the realisation of a metamorphic antenna, using a low cost photoconductive layer under realistic levels of illumination, would be extremely difficult to achieve. This is because the photoconductivity is low if the large area

fabrication techniques (such as thick film deposition) needed for antenna applications are used. A porous morphology limited the maximum conductivity obtainable [1].

Consequently a different approach to implement a metamorphic antenna was investigated in the second year of the project. In this approach small area semiconductors were used as switches between the conducting elements of segmented apertures or antennas (as illustrated in Figure 4). Altering the combination of ON and OFF switch settings creates different antenna shapes with correspondingly different antenna properties. By using small areas of photoconducting semiconductor this later approach offers two advantages over the earlier, large-area, photoconducting layer approach: firstly a monocrystal semiconductor can be used, providing high mobility and conductivity; secondly the total optical power requirement for switching should be considerably reduced.

A metamorphic antenna would primarily offer future systems a rapidly and electronically reconfigurable antenna providing: (a) wide frequency coverage

from several instantaneously narrower bands; (b) versatile radiation patterns, potentially with some beam pointing capability [2]. The antenna properties could be changed dynamically, as driven by requirements, or adaptively, in response to alterations in the environment.

Technical Programme

Approaches for reconfigurable antennas have largely considered mechanical MEMS switches or electronic devices such as PIN diodes or FETs [2]. It was the purpose of this project mainly to investigate the suitability of photoconducting semiconductors in a metamorphic, segmented antenna structure. Optically activated switches could offer the benefit that bias lines, which can reduce antenna performance if included on the antenna plane, are not required. The technical programme included the following steps:

- Design and assessment of an ideal segmented antenna, in which conducting square pads are connected by perfectly conducting links, to act as a baseline for subsequent work.
- Solid state physics modelling to predict semiconductor electrical properties relevant to antenna performance, including optical density, conductivity and dielectric constant.
- Electromagnetic modelling and assessment of the performance of a switched segmented antenna incorporating photoconducting switches, utilising the results from the above semiconductor modelling, and comparison with the ideal segmented antenna from the first step.
- Design, fabrication, measurement and evaluation of first microstrip and antenna structures containing photoconducting switches.

Ideal segmented antenna properties

A bowtie antenna was selected as an example segmented antenna, since it offers broadband operation and a simple structure for evaluating switching concepts. An ideal segmented antenna was designed to cover a frequency range of approximately 7 to 13GHz and is shown in Figure 1. The antenna comprised perfectly conducting square pads, some of which were connected by perfectly conducting links to form an antenna shape.

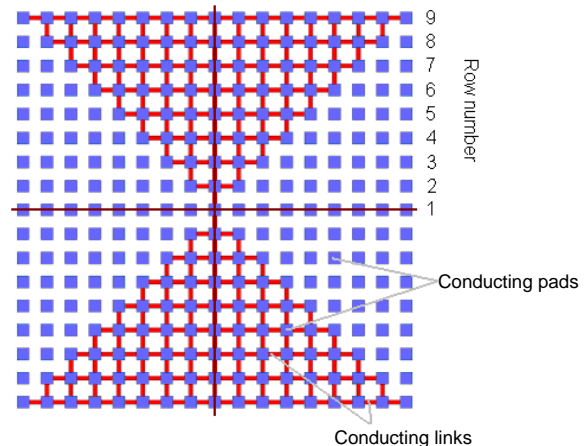


Figure 1 Ideal segmented antenna

The return loss predicted by electromagnetic modelling for four states of the antenna is given in Figure 2, indicating that a broad frequency coverage could be obtained from contiguous narrower bands. Disconnected pads remained in the model.

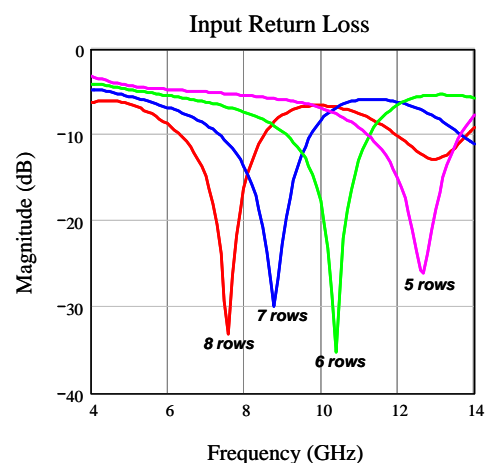


Figure 2 Return loss versus frequency for the four antenna states in which between 5 and 8 rows are connected in each arm of the bowtie. Radiation patterns were also predicted; the gain variation from the states over 7-13GHz

was less than 1dB. The properties of a continuous sheet antenna, equivalent to the antenna state with 6 rows connected in each arm, were also modelled. The gain of the continuous and segmented antennas compared well, with the gain of the latter being only 1.5dB lower. The segmented antenna resonated at a lower frequency than continuous one (by about 1.7GHz).

Semiconductor modelling

Options for the photoconducting semiconductor include Si, CdS and GaAs. Silicon was chosen for first investigations since an off-the-shelf monocrystal giving a high mobility was readily available to construct structures for measurements.

A solid-state physics model, an extension of that from the first year of the project [1], was used to predict photoconductor properties for incorporation in subsequent electromagnetic modelling. Carrier concentration was first calculated as a function of optical illumination intensity, assuming generation of one electron-hole pair per incident photon and an illumination wavelength of 980nm. This wavelength is known to provide a balance between an acceptable absorption coefficient and efficient carrier generation. Of the available grades, high resistivity silicon (2000-9000Ωcm) was assumed, to provide a low carrier density and high resistance for the switch OFF state. Conductivity and complex permittivity were calculated from the carrier concentration, linking them directly to illumination intensity. Results are given in Table 1. As expected, the carrier concentration, conductivity and $\tan \delta$ all increase with increasing illumination, while the dielectric constant decreases.

The proportion of incident optical power transmitted as a function of silicon thickness is shown in Figure 3 for an assumed absorption coefficient of 100cm^{-1} . This indicates that switches with a thickness

greater than 0.1mm should be used to maximise performance.

Optical Intensity (mW/cm ²)	Carrier concn. (cm ⁻³)	Conductivity (Sm ⁻¹)	Dielectric constant	Tan delta
0	1×10^{12}	0.1	11.9	0.02
1	3×10^{13}	1.4	11.9	0.02
10	2×10^{14}	6.9	11.4	2.12
100	3×10^{15}	95.1	10.8	32.02
1000	2×10^{16}	557.3	6.8	293.9

Table 1 Predicted silicon properties as a function of illumination intensity

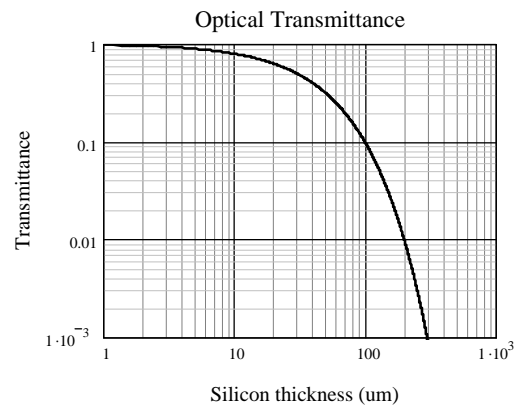


Figure 3 Optical transmittance versus thickness

Switched segmented antenna properties

A switched segmented bowtie antenna incorporating silicon switches was designed and modelled to compare its properties with those of the ideal segmented antenna. The top half of the antenna is illustrated in Figure 4. It was designed for a centre frequency of 1.2GHz and included conducting links with gaps bridged by silicon pieces. Properties were predicted for the following states: (a) no switches present, but gaps in the links; (b) continuous, perfectly conducting links; (c) silicon switches illuminated by an optical power density of 1mWcm^{-2} , to represent an OFF state; (d) silicon switches illuminated by optical power densities of 100 and 200 mWcm^{-2} , to represent ON states. The semiconductor properties determined above were included in the electromagnetic model to represent the Si switches.

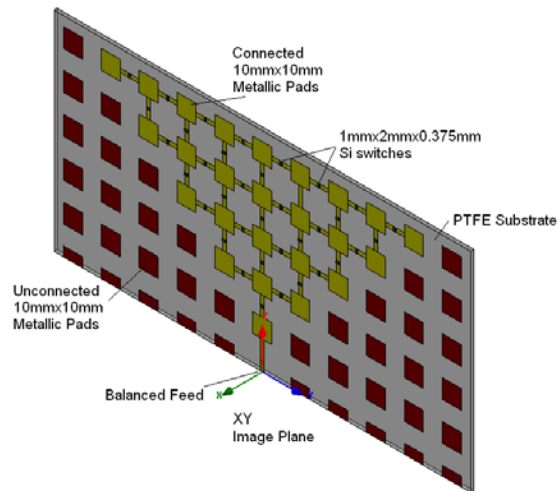


Figure 4 Top half of a switched segmented bowtie antenna

The return loss as a function of frequency for the above states is shown in Figure 5. Also shown is the return loss predicted for an equivalent continuous sheet antenna.

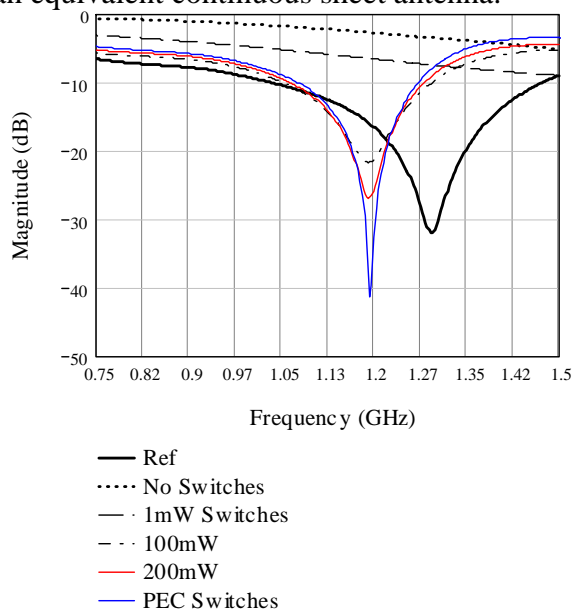


Figure 5 Return loss versus frequency for a switched segmented and reference antenna

With no switches present, but gaps in the links, there is no resonance and a high return loss. With switches present in the OFF state there is also no resonance, but the return loss is now lower. Continuous conducting links give a resonance with low return loss, as do the switches when present and in the ON state. The resonance of the switched segmented antenna is at a lower frequency than that of the equivalent

continuous antenna, as found previously for the ideal segmented antenna. The same gain was obtained for switches in the ON state and continuous links.

The above results together indicate that: (a) it may be possible to use photoconducting switches as a mechanism to change antenna states; (b) the predicted gain of a segmented antenna compares well with that of an equivalent continuous antenna, being only ~ 1.5 dB lower.

Evaluation structures

Structures with a small number of switches were used for first evaluations. Two simple structures were defined to measure switch and switched-state antenna properties: (a) a silicon switch bridging a gap in a microstrip line (Figure 6); (b) a dipole antenna containing several switches, one in an arm and three in a balun (Figure 8). Changing a dipole resonant frequency with switches had been reported previously and so was not investigated here [3].

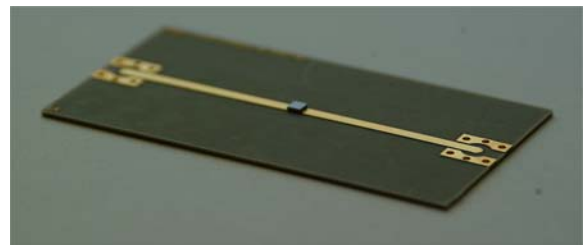


Figure 6 Evaluation structure with silicon switch bridging a gap in microstrip line

The microstrip evaluation structure had a track with a width of 2mm and a gap of 0.4mm bridged by a $2 \times 1 \times 0.525$ mm (width by length by height) silicon switch. Figure 7 shows the predicted proportions of input power reflected (S_{11}) and transmitted (S_{12}) as a function of incident optical power density. As the optical power is increased the structure becomes transmitting, changing from an S_{12} of -22 to -1 dB.

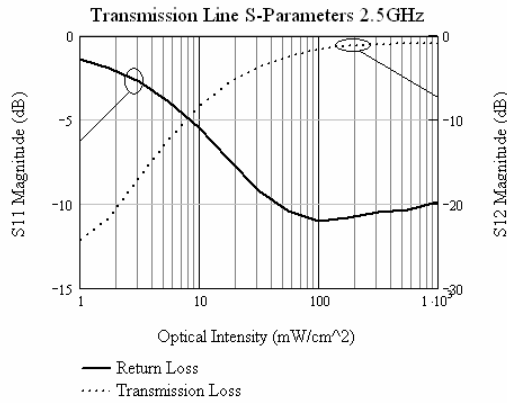


Figure 7 Predicted return loss (S_{11}) and transmission loss (S_{12}) of the microstrip structure versus optical power density

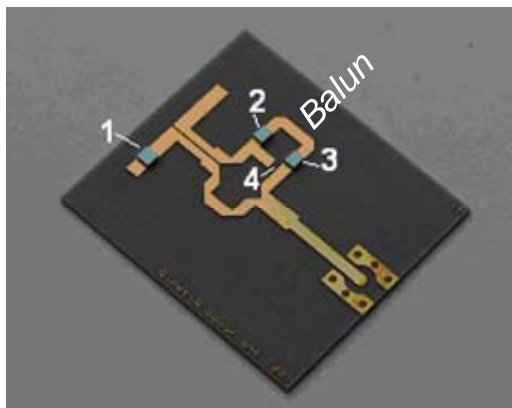


Figure 8 Evaluation structure with a dipole and switchable balun

The dipole structure constituted a dipole designed to resonate at about 8.0 GHz and a switchable balun feed. Switches 2, 3 and 4 (the last not shown in Figure 8) are intended to control the balun, switching it between a normal state that allows the dipole to operate as an efficient antenna and another state that prevents the antenna radiating.

For these first structures, the switches shown in Figures 6 and 8 were cut from a high resistivity silicon wafer (as assumed for the modelling), using a diamond saw. They were mounted onto the metallic strips of the structures with conductive epoxy, using careful procedures intended to prevent voids or bridging across the gap.

Evaluation

Measurements of the first structures were made with a solid state laser beam widened to illuminate all the switches. The switches were illuminated on their upper surface (i.e. opposite the substrate). Light barriers were placed over appropriate areas to provide OFF states. The laser and the experimental set-up allowed the optical power incident on the switches to be varied.

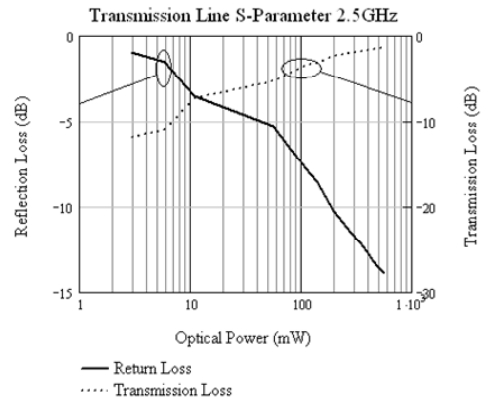


Figure 9 Measured return loss (S_{11}) and transmission loss (S_{12}) of the microstrip structure

The measured S_{11} and S_{12} of the microstrip line structure as a function of total optical power incident on the switch is shown in Figure 9, which should be compared with Figure 7. Figure 9 shows that the switch could be successfully changed from an OFF to an ON state, but that a substantially higher optical power than predicted ($\sim 200 \text{ mW/mm}^2$) was required to generate the ON state. The difference between prediction and experiment was attributed in part to two simplifying assumptions made to complete the modelling. These were that: (a) the carrier diffusion length was about 1.0mm (a typical value for silicon) leading to a uniform carrier density throughout the switch; (b) there was a loss-less interface between the switch and microstrip line. In practice, the carrier density may have a profile, with the highest concentration near the upper surface opposite the microstrip line. This could be caused by a reduction in carrier lifetime due to, for example, surface effects. Further differences between measurement and prediction could have

been due to the laser wavelength, which was 20nm lower than the 980 nm used for modelling, sufficient to cause generation of considerably fewer carriers than predicted.

It is believed that the dominant mechanism limiting the photoconductive efficiency of the devices was trapping and recombination of the photo-generated carriers at defect sites on the surfaces of the silicon switches, since diamond-sawing can carry a high density of damage-induced surface defects. For subsequent work a large decrease in defect density – by perhaps 4 orders of magnitude – could be achieved by using reactive ion etching in place of sawing, and by applying sequential oxidise/etch cycles to polish the surface. It is anticipated that with this more elaborate process, surface recombination would no longer be dominant and the carrier lifetime and optical input power requirement might improve by 1-2 orders of magnitude.

Measurements of the dipole structure found a return loss of -30dB at resonance when the switches in the balun was set to allow the antenna to radiate efficiently, and a return loss of -2dB when they were set to prevent radiation. The measured values agreed well with predictions, indicating that optically activated switches could be incorporated into effective antenna control structures to change states.

Summary and conclusions

This work has considered the use of photoconducting semiconductor switches in metamorphic segmented antennas, using silicon as an example. Bowtie antennas were designed and modelled; results giving a broad frequency coverage, formed from switching between narrower contiguous bands, were obtained.

Two simple structures were designed and fabricated for first experimental evaluations. A microstrip line, with a

silicon switch bridging a gap in the line, was successfully changed from an OFF to an ON state, but an optical power density of $\sim 200\text{mW}/\text{mm}^2$ was needed to achieve this fully. It is anticipated that this power could be reduced using a more elaborate silicon switch preparation process. Results for a dipole structure containing a switchable balun indicated that optically activated switches could be incorporated into effective antenna control structures to change states. Ways forward for this work would include: (a) investigation of methods to lower the optical power required to switch silicon; (b) consideration of alternative semiconductors; (c) optical feed and control techniques.

References

1. Tuffin RP, Sage IC, Hughes BJ, Ball GJ, *Electronically Controlled Metamorphic Antenna*, EMRS DTC 4th Annual Technical Conference, Edinburgh, July 2007.
2. Pringle LN, Harms PH, Blalock SP, Kiesel GN, Kuster EJ, Friederich PG, Prado RJ, Morris JM, Smith GS, *A Reconfigurable Aperture Antenna Based on Switched Links Between Electrically Small Metallic Patches*, IEEE Trans AP, Vol. 52, No. 6, June 2004.
3. Panagamuwa CJ, Chauraya A, Vardaxoglou JC, *Frequency and Beam Reconfigurable Antenna Using Photoconducting Switches*, IEEE Trans AP, Vol. 54, No. 2, February 2006.

Acknowledgements

The work reported in this paper was funded by the Electro-Magnetic Remote Sensing (EMRS) Defence Technology Centre, established by the UK Ministry of Defence and run by a consortium of SELEX Galileo, Thales UK, Roke Manor Research and Filtronic.